Published in final edited form as:
Eur J Neurosci. 2010 April ; 31(7): 1219–1232. doi:10.1111/j.1460-9568.2010.07156.x.

Substance P modulation of TRPC3/7 channels improves respiratory rhythm regularity and ICAN-dependent pacemaker activity

Faiza Ben-Mabrouk[1] and **Andrew Kieran Tryba**[1,*]

[1]Dept of Physiology, Medical College of Wisconsin, 8701 Watertown Plank Rd., Milwaukee, WI 53226

Abstract

Neuromodulators, such as Substance P (SubP) play an important role in modulating many rhythmic activities driven by central pattern generators (e.g., locomotion, respiration). However, the mechanism by which SubP enhances breathing regularity has not been determined. Here, we used mouse brainstem slices containing the pre-Bötzinger Complex (Pre-BötC) to demonstrate, for the first time, that SubP activates transient receptor protein canonical (TRPC) channels to enhance respiratory rhythm regularity. Moreover, SubP enhancement of network regularity is accomplished *via* selective enhancement of ICAN-dependent intrinsic bursting properties. In contrast to INaP-dependant pacemakers, ICAN-dependant pacemaker bursting activity is TRPC dependent. Western Blots reveal TRPC3 and TRPC7 channels are expressed in rhythmically active ventral respiratory group (VRG) island preparations. Taken together, these data suggest that SubP-mediated activation of TRPC3/7 channels underlies rhythmic ICAN-dependent pacemaker activity and enhances the regularity of respiratory rhythm activity.

Introduction

Neural networks termed central pattern generators (CPG) underlie rhythmic motor activities such as gut peristalsis, locomotion and breathing (Smith et al., 1991b; Grillner, 2006). Synaptic and intrinsic membrane conductances are continuously modulated by excitatory and inhibitory inputs coming from different regions of the brain (Barthe and Clarac, 1997; Thoby-Brisson and Simmers, 1998; Gray et al., 1999; Feldman et al., 2001; Kozlov et al., 2001; Jun et al., 2004; Pearlstein et al., 2005; Tryba et al., 2006; Saideman et al., 2007; Boesmans et al., 2008; Chevalier et al., 2008) giving an important plasticity to the network. In mammals, it is well established that, the pre-Bötzinger Complex (pre-BötC) located within the medullary ventral respiratory group (VRG) is critical for generating the inspiratory rhythm activity (Gray et al., 2001; Wenninger et al., 2004; McKay et al., 2005). This rhythm depends on both a non specific cation current (ICAN) and persistent sodium current (INaP) (Thoby-Brisson and Ramirez, 2001; Peña et al., 2004; Pace et al., 2007). The pre-BötC can be isolated *in vitro*, and generate the three forms of the respiratory pattern, the normal respiratory activity (eupneic activity), sighs and gasping (during hypoxic conditions) (Lieske et al., 2000). These three patterns are strongly influenced by neuromodulators (Lieske et al., 2000; Ruangkittisakul et al., 2008; Tryba et al., 2008).

[*]Corresponding author: Medical College of Wisconsin Dept. of Physiology 8701 Watertown Plank Rd. Milwaukee WI 53051 Phone: 414.456.4975 FAX: 414.456.6546 atryba@mcw.edu .

Because of the important role of neuromodulators, a disturbance in the neuromodulatory system may lead to breathing disorders such as Rett syndrome or Suddent Infant Death Syndrome (SIDS). In these cases, respiratory irregularities are associated with a deficiency in numerous neuromodulators, such as serotonin, dopamine, noradrenaline and Substance P (Lekman et al., 1989; Zoghbi et al., 1989; Matsuishi et al., 1997; Segawa, 1997; Deguchi et al., 2000; Viemari et al., 2005b).

In our study we focused on the excitatory effects of SubP on the respiratory rhythm activity. SubP activates neurokinin-1 (NK-1) receptors (Gray et al. 1999) that are positively coupled to G q/11-proteins, that are pertussis toxin-insensitive and will activate phospholipase C (PLC), leading to the production of diacylglycerol (DAG) and inositol triphosphate (IP3) and activation of PKC. This intracellular pathway is known to induce a cation current. However, the nature of channels opened by SubP is not yet known.

Here we propose that SubP activates TRP channels (TRPCs) to improve the regularity of respiratory rhythmic activity. TRPCs are non selective cation channels that are permeable to monovalent and divalent ions (Clapham, 2003). Some of the TRPCs are activated by the inositol phospholipid hydrolysis system. Also, the SubP receptor can be functionally linked to TRPC3 channels (Oh et al., 2003). Our results reveal that SubP activates TRPC3 and/or TRPC7 (TRPC3/7) channels that underlies rhythmic ICAN-dependant pacemaker activity and enhances the regularity of the respiratory rhythm.

Materials and Methods

All experiments conformed to the guiding principles for the care and use of animals approved by the National Institutes of Health (U.S.A.) and the Internal Animal Care and Use Committee at the Medical College of Wisconsin.

Respiratory medullary brain-slice preparation

All experiments used the transverse, rhythmic 600μm thick medullary brain-slice obtained from 8-11 day old, CD-1 outbred mice (Charles River Laboratories, Wilmington, MA) (Smith et al., 1991a). CD-1 mice were quickly decapitated at the C3/C4 spinal level and the brain-stem was dissected in ice cold artificial cerebral spinal fluid (ACSF) that was equilibrated with carbogen (95% O_2 and 5% CO_2, pH=7.4). Rhythmic medullary brainslice preparations (600μm thick) containing the ventral respiratory group (VRG), including the pre-Bötzinger Complex (pre-BötC), were obtained by slicing the medulla using a microslicer (Leica, VT1000S, Nussloch, Germany) as described in detail elsewhere (Thoby-Brisson and Ramirez, 2001; Chevalier et al., 2008). Slices were submerged in a recording chamber (6 mL) under circulating ACSF (30°C; flow rate 17 ml/min, total circulating volume = 200mL).

The ACSF contained in mM: 118 NaCl, 3 KCl, 1.5 $CaCl_2$, 1 $MgCl_2$*$6H_2O$, 25 $NaHCO_3$, 1 NaH_2PO_4 and 30 D-glucose, equilibrated with carbogen (95% O_2 and 5% CO_2, pH = 7.4). All ACSF chemicals were obtained from Sigma (St. Louis, MO, U.S.A.). Extracellular KCl was elevated from 3mM to 8mM over a span of 30 minutes before commencing recordings to maintain rhythmic population activity (Tryba et al., 2003). Note that raising ACSF $[K^+]_o$ does not artificially introduce pacemaker bursting properties; pacemakers show similar bursting properties in 3mM versus 8mM $[K^+]_o$ ACSF (Tryba et al., 2003). Further, it should be noted that $[K^+]_o$ changes on a breath by breath basis, however these changes in $[K^+]_o$ do not obviously alter the form of respiratory activity generated, as both eupneic and gasping activities can be recorded in hypokalemic and hyperkalemic conditions *in situ* (St.-John et al., 2005). As bath temperature can alter respiratory slice activity (Tryba and Ramirez, 2004a), bath temperature was monitored and maintained at 30°C ± 0.7°C using a Warner

Instrument Corp. (Hamden, CT) TC-344B temperature regulator with an in-line solution heater (SH-27B); bath temperature at various locations within the bath was uniform.

Western Blots of VRG- islands containing the pre-BötC

In order to determine the expression of TRP channels and NK-1 receptors in the VRG, we made rhythmic 600μm thick VRG-island preparations (Johnson et al., 2001) containing the pre-BötC by taking a brainslice preparation (above) and cutting a wedge-shaped piece of tissue containing the pre-BötC out of the transverse brainslice using a sharp scalpel blade (Tryba et al., 2008). The extent of the VRG-island/pre-BötC to be removed was determined by delineating the VRG boarders with population electrode mapping on the surface of the slice prior to cutting out the VRG-island. We also isolated the cortex and cerebellum, as a positive control for TRP channel expression. Tissues were homogenized in a 10mM potassium phosphate buffer, pH=7.7, containing complete mini protease inhibitor (0.36 mg/mL) (Roche, 400USA) added at time of use. The homogenates were centrifuged at 4600 rpm for 15 min at 4°C. Protein concentrations in the supernatant were determined using a DC protein assay (Bio-Rad Labs, Hercules, CA, USA). Proteins were loaded in either 10μg, 15 μg, or 50μg amounts in each well and separated by electrophoresis on a 10% Tris-HCl Ready Gel (Bio-Rad Labs, Hercules, CA, USA) at 100 V under denaturing conditions. Proteins were then transferred to a nitrocellulose membrane (Bio-Rad Labs, USA). The membranes were blocked overnight at +4°C with 5% non-fat dried milk (Bio-Rad Labs, USA) and 1% albumin from bovine serum (Sigma, USA) in Tris Buffered Saline, pH 7.5, containing 0.1% Tween-20 (TBS-T) and immuno-blotted for 2h at room temperature with either anti-NK1 antibody (1:10000) (Invitrogen, USA) or anti-TRPC1 antibody (1:500) (Alomone labs, Israel), or anti-TRPC3 antibody (1:500) (Alomone labs, Israel) or anti-TRPC4 antibody (1:100) (Alomone labs, Israel), or anti-TRPC5 antibody (1:300) (Santa Cruz, USA), or anti-TRPC6 antibody (1:400) (Alomone labs, Israel), or anti-TRPC7 antibody (1:300) (Millipore, USA), anti-TRPM4 antibody (1:1000) (Abcam, USA) in 2% NFDM in TBS-T, anti-GAPDH (1:300) (Abcam, USA) used as a loading control. The secondary antibody, goat anti-rabbit-HRP (1:10000) (Santa Cruz, CA, USA) was incubated for 1h at room temperature. Membranes were developed using enhanced chemiluminescence (Pierce ECL-West Pico kit, Thermo Fisher Scientific, Pittsburgh, PA, USA) on X-ray film (Phenix Research Products, Candler, NC, USA).

Electrophysiology- Population activity and identification of inspiratory neurons

Extracellular recordings were obtained with glass suction electrodes positioned on the slice surface in the ventral respiratory group (VRG) near or on top of the preBötC (Figs. 1A, 1B). The VRG population bursting is dominated by inspiratory neurons such that integrated VRG (∫VRG) activity is in-phase with integrated XII (∫XII) activity (Tryba et al., 2006; Chevalier et al., 2008). Thus, VRG population bursts serve as a marker of fictive inspiration (Tryba et al., 2006; Chevalier et al., 2008). This population activity was rectified and integrated and the data were digitized with a Digidata acquisition system (Molecular Devices, CA), stored on an IBM compatible PC using Axoscope 10 (Molecular Devices, CA) software and analyzed off-line using Igor Pro (WaveMetrics, Lake Oswego, OR).

Intracellular whole cell current-clamp recordings were obtained with a MultiClamp 700B amplifier (Molecular Devices, CA), applying the blind-patch technique to VRG neurons in brainstem slice preparations (Thoby-Brisson and Ramirez, 2001). Patch electrodes were manufactured from filamented borosilicate glass tubes (Clark G150F-4; Warner Instruments Corp., Hamden, CT, USA) and filled with an intracellular solution containing (in mM): 140 K-gluconic acid, 1 $CaCl_2$*$6H_2O$, 10 EGTA, 2 $MgCl_2$*$6H_2O$, 4 Na_2ATP, 10 HEPES.

Only inspiratory VRG neurons active in-phase with the ʃVRG population burst were recorded in this current-clamp study (Fig.1B). The discharge pattern of each cell type was first identified in the cell-attached mode and remained similar in whole-cell configuration (Peña et al., 2004;Tryba et al., 2008). Experiments were then performed in the whole cell patch-clamp mode. The Vm values were corrected for the liquid junction potential as calculated using pClamp 10 software (Molecular Devices). In current-clamp, neurons were isolated from ionotropic chemical synaptic input using a mixture of glutamatergic, GABAergic and glycinergic antagonists. These drugs were bath applied at the final concentrations of: 20μM 6-cyano-7-nitroquinoxaline-2,3-dione (CNQX (Tocris Biosciences, Ellisville MO, USA)), 10 μM (RS)-3-(2-Carboxypiperazin-4-yl)-propyl-1-phosphonic acid ((RS)-CPP)(Tocris Biosciences), 1 μM Strychnine (Sigma) and 20 μM bicuculline free-base (Sigma Aldrich). Note that unlike bicuculline methiodide, the bicuculline free base derivative is a specific GABA receptor antagonist that does not block apamin-sensitive Ca^{2+}-activated K^+ currents. Substance P (Sigma) was bath-applied at 0.1 μM, SKF-96365 Hydrochloride (Tocris Biosciences) was bath-applied at 5-10μM, flufenamic acid (FFA) at 50 μM, riluzole (Sigma) was bath-applied at 10 μM.

A subset of neurons, considered inspiratory pacemakers, continued to generate voltage-dependent intrinsic bursting properties following blockade of ionotropic glutamate (both AMPAR and NMDAR antagonists were co-applied) and after blocking GABA and glycinergic receptors (Peña et al., 2004). These pacemakers met several criteria before being classified as inspiratory pacemaker neurons; the criteria used here are provided in detail elsewhere (Thoby-Brisson and Ramirez, 2001; Tryba et al., 2003). In control conditions, in contrast to nonpacemakers, brief depolarizing current injection could evoke an additional cellular burst that was ectopic relative to ʃVRG population bursts. Unlike pacemakers, hyperpolarization of nonpacemakers below threshold caused nonpacemakers to cease bursting (Tryba et al., 2003). After isolation of the neuron from fast chemical synaptic input with bath applied CNQX, CPP, strychnine and bicuculline, pacemakers continued to burst in absence of ʃVRG population bursts. Second, isolated pacemakers exhibited voltage-dependent bursting properties. That is, brief depolarizing current injection could evoke a burst, or hyperpolarizing current could terminate an ongoing burst; either of these reset the ongoing pacemaker bursting rhythm. Finally, depolarizing current injection increased, and injected hyperpolarizing current injection decreased, the bursting frequency.

Data analysis

To measure ʃVRG network or pacemaker bursting regularity, we calculated an irregularity score (S), by applying a formula for consecutive cycle length values: Sn = 100 * ABS(Pn-Pn-1)/Pn-1, where Sn = score of the nth cycle, Pn being its period, Pn-1 the period of the preceding burst and ABS the absolute value (Barthe and Clarac, 1997; Telgkamp et al., 2002; Viemari et al., 2005a; Chevalier et al., 2008). Regular rhythms have lower irregularity scores while irregular rhythms have higher irregularity scores (Telgkamp et al., 2002; Chevalier et al., 2008). For comparison, we calculated the irregularity score of the ʃVRG and inspiratory neurons (over a period of 5mins) and isolated pacemaker rhythmic bursts (over a period of 2mins) in control and following experimental manipulation. The burst area was measured as the area between the baseline and the burst envelope, while frequency was calculated based on the burst peak intervals. To minimize the potential influence of baseline fluctuations and differences in burst peak trajectories, the burst duration was calculated as the duration of the burst at half-maximal burst amplitude.

Data were analyzed off-line with ClampFit 9.2 (Molecular Devices), Igor Pro (WaveMetrics, Lake Oswego, OR) and further statistical analysis was performed with Graph Pad Prism software v4.03 (San Diego, CA). A paired Student’s t-test was used to compare raw data obtained from a given specimen in two different conditions. Results are given in

the text in the form of mean (*m*) ± standard error and in the figures the data are represented in the form of % of control (significance was assumed for values $p \leq 0.05$).

Results

Mechanisms underlying Substance P (SubP) modulation of eupneic activity

TRPC channel antagonists block SubP-mediated enhancement of fictive eupnea—SubP enhances the regularity of fictive eupneic activity *in vitro* (Telgkamp *et al*. 2002; Peña and Ramirez 2004), however the underlying mechanism is unknown. SubP has been shown to activate TRPC3 channels in HEK293 cells, leading to an inward non-specific cation current (ICAN) (Oh et al. 2003). Here, we test the hypothesis that SubP enhances fictive eupneic regularity and bursting properties *via* TRPC channel activation using the respiratory medullary brainslice preparation, containing the Pre-BötC. We bath-applied 0.1 μM SubP for 20mins., evoking a decrease in fictive eupnea irregularity (m=0.35 ± 0.05 and m= 0.17 ± 0.01, before and after SubP, respectively, n= 20 slice preparations, p<0.001, paired t-test), enhancement of ∫VRG burst area (m=0.09 ± 0.02 and m= 0.17 ± 0.07, before and after SubP, respectively, n= 20 slice preparations, p<0.05, paired t-test) and increase in burst frequency (m=0.21 ± 0.02 and m= 0.36 ± 0.02, before and after SubP, respectively, n= 20 slice preparations, p=0.001, paired t-test) without altering burst duration (m=0.51 ± 0.02 and m= 0.50 ± 0.03, before and after SubP, respectively, n= 20 slice preparations, p>0.05, paired t-test) (Figs. 2A1-2, 2B). These data are consistent with previously published studies of SubP effects on respiratory activity (Gray et al., 1999; Shvarev et al., 2002; Peña and Ramirez, 2004). After slices were exposed to SubP for 20mins, we co-applied a TRPC channel antagonist (Zhu et al. 1998), SKF-96365. Here, we discovered that SubP-mediated enhancement of respiratory activity (Figs. 2A1-2; 2B; 3A1-A2) is reversed by subsequent bath-application of the TRPC channel antagonist, SKF-96365 (Amaral and Pozzo-Miller, 2007). The ∫VRG burst irregularity increases (m=0.17 ± 0.02 and m= 0.30 ± 0.05, SubP and SubP + SKF-96365, respectively, n= 11 slice preparations, p<0.05, paired t-test) and decreases burst area (m=0.17 ± 0.05 and m= 0.11 ± 0.04, under SubP and SubP + SKF-96365, respectively, n= 11 slice preparations, p<0.01, paired t-test), burst duration (m=0.48 ± 0.03 and m= 0.41 ± 0.04, SubP and SubP + SKF-96365, respectively, n= 11 slice preparations, p<0.01, paired t-test) and frequency (m=0.39 ± 0.04 and m= 0.35 ± 0.06, SubP and SubP + SKF-96365, respectively, n= 11 slice preparations, p<0.05, paired t-test) (Figs. 3A1;3A2; 3B1;3B2). After bath-application of SKF-96365, additionally blocking the persistent sodium current (INaP) with riluzole completely abolished the ∫VRG respiratory rhythm (Fig. 3C; n=11 slice preparations; in n=11/11) whereby no rhythmic activity was recorded for >17mins.

While SubP-enhances fictive eupnea, subsequent bath-application of SKF-96365 effectively restores ∫VRG bursting regularity (m=0.31 ± 0.06 and m= 0.30 ± 0.05, before and after bath application of SubP + SKF-96365, respectively, n= 11 slice preparations, p>0.05, paired t-test), burst area (m=0.07 ± 0.03 and m= 0.11 ± 0.04, before and after bath application of SubP + SKF-96365, respectively, n= 11 slice preparations, p>0.05, paired t-test) and frequency (m=0.24 ± 0.04 and m= 0.35 ± 0.06, before and after bath application of SubP + SKF-96365, respectively, n= 11 slice preparations, p>0.05, paired t-test) to control levels (ACSF alone), while burst duration (m=0.47 ± 0.03 and m= 0.41 ± 0.045, before and after bath application of SubP + SKF-96365, respectively, n= 11 slice preparations, p<0.01, paired t-test) is reduced following SKF-96365 application (Fig. 3D). Thus, SubP-mediated modulation of TRPC channels plays a major role in altering fictive eupnea regularity.

ICAN antagonists block SubP-mediated enhancement of fictive eupnea

We tested the role of ICAN in SubP-mediated enhancement of fictive eupneic activity by blocking ICAN with using FFA (50μM), which in HEK293 cell lines, was shown to block TRPC3 channels (Zhou et al., 2008). After bath-applying SubP for 20mins., subsequent co-application of FFA increases ∫VRG burst irregularity (m= 0.17 ± 0.02 and m= 0.45 ± 0.09, before and after perfusion of FFA, n= 6 slice preparations, p<0.05, paired t-test) and decreases burst area (m= 0.13 ± 0.04 and m= 0.04 ± 0.019, before and after perfusion of FFA, n= 6 slice preparations, p<0.001, paired t-test), duration (m= 0.54 ± 0.05 and m= 0.4 ± 0.04, before and after perfusion of FFA, n= 6 slice preparations, p<0.01, paired t-test) and frequency (m= 0.25 ± 0.03 and m= 0.14 ± 0.05, before and after perfusion of FFA, n= 6 slice preparations, p<0.01, paired t-test) (Figs. 4A1-A2; Figs. 4B1-B2). Additionally applying riluzole completely abolishes fictive eupneic rhythmic activity (∫VRG) (Fig. 4C; n=6 slice preparations; in n=6/6, no rhythmic activity was recorded for >17mins.). Interestingly, the effects of FFA on the SubP response, effectively restores ∫VRG burst irregularity (m= 0.43 ± 0.13 and m= 0.45 ± 0.09, before and after perfusion of SubP + FFA, n= 6 slice preparations, p>0.05, paired t-test) burst area (m= 0.08 ± 0.04 and m= 0.04 ± 0.01, before and after perfusion of SubP + FFA, n= 6 slice preparations, p>0.05, paired t-test) and burst frequency (m= 0.55 ± 0.05 and m= 0.4 ± 0.04, before and after perfusion of SubP + FFA, n= 6 slice preparations, p>0.05, paired t-test) to similar values that were observed in ACSF alone, while burst duration shortens (m= 0.06 ± 0.03 and m= 0.14 ± 0.05, before and after perfusion of SubP + FFA, n= 6 slice preparations, p<0.001, paired t-test) (Fig. 4D). Taken together these data demonstrate that the SubP-mediated enhancement of fictive eupneic can be blocked by TRPC channel antagonists.

In additional experiments, we examined the role of endogenous TRPC channel activity by bath-applying 50μM FFA (alone, in absence of exogenous SubP) during fictive eupnea. Bath-application of FFA increases ∫VRG population bursting irregularity (m= 0.26 ± 0.04 and m= 0.42 ± 0.08, before and after perfusion of FFA, n= 5 slice preparations, p<0.01, paired t-test) and decreases burst area (m= 0.04 ± 0.01 and m= 0.03 ± 0.004, before and after perfusion of FFA, n= 5 slice preparations, p<0.05, paired t-test), and reduces burst frequency (m= 0.30 ± 0.04 and m= 0.21 ± 0.06, before and after perfusion of FFA, n= 5 slice preparations, p<0.05, paired t-test) but does not alter burst duration (m= 44 ± 0.02 and m= 0.31 ± 0.04, before and after perfusion of FFA, n= 5 slice preparations, p>0.5, paired t-test) (Figs. 5A1-5A2; graph not shown). In the presence of FFA, subsequent co-application of 0.1μM SubP fails to decrease the ∫VRG irregularity (m= 0.42 ± 0.08 and m= 0.36 ± 0.07, in FFA and in FFA + SubP, respectively, n= 5 slice preparations, p>0.05, paired t-test), burst area (m= 0.03 ± 0.004 and m= 0.03 ± 0.003, in FFA and in FFA + SubP, respectively, n= 5 slice preparations, p>0.05, paired t-test) and burst duration (m= 0.31 ± 0.04 and m= 0.32 ± 0.04, in FFA and in FFA + SubP, respectively, n= 5 slice preparations, p>0.05, paired t-test). However, network bursting frequency increases (m= 0.21 ± 0.06 and m= 0.40 ± 0.06, in FFA and in FFA + SubP, respectively, n= 5 slice preparations, p>0.05, paired t-test) (Figs. 5B1-5B2) which may be due to SubP enhancement of other (non-TRPC channel mediated) intrinsic and/or synaptic mechanisms, such as enhancement of NMDAR activity (Peña and Ramirez, 2004). Subsequent co-application of riluzole eliminates the ∫VRG respiratory rhythm (n=5 slice preparations, Fig. 5C; in n=5/5, no rhythmic activity was recorded for >17mins). The ∫VRG rhythmic activity during co-application of SubP and FFA remained more irregular (m= 0.26 ± 0.04 and m= 0.36 ± 0.07, before and after perfusion of FFA + SubP, n= 5 slice preparations, p<0.05, paired t-test), with a smaller burst area (m= 0.04 ± 0.01 and m= 0.03 ± 0.03, before and after perfusion of FFA + SubP, n= 5 slice preparations, p<0.01, paired t-test) than observed in ACSF alone while burst duration (m= 0.44 ± 0.02 and m= 0.32 ± 0.04, before and after perfusion of FFA + SubP, n= 5 slice preparations, p>0.05, paired t-test) and frequency (m= 0.30 ± 0.04 and m= 0.40 ± 0.06, before and after perfusion

of FFA + SubP, n= 5 slice preparations, p>0.05, paired t-test) are similar to control values (Fig. 5D). These data demonstrate the importance of ICAN in SubP-mediated enhancement of fictive eupneic regularity.

Blocking INaP does not alter SubP-enhanced fictive eupneic regularity—To test whether blocking INaP, prevents SubP effects on fictive eupnea, we first bath-applied 0.1μM SubP for 20mins., evoking a decrease in fictive eupneic irregularity, enhancement of ∫VRG burst area and an increase in burst frequency, without altering burst duration (Figs. 2B; 6A1-6A2). Subsequent bath application of riluzole does not alter the SubP-enhanced respiratory rhythm regularity (m= 0.14 ± 0.02 and m= 0.16 ± 0.04, in SubP and in SubP + riluzole, n= 6 slice preparations, p>0.05, paired t-test) or ∫VRG burst area (m= 0.32 ± 0.17 and m= 0.24 ± 0.13, in SubP and in SubP + riluzole, n= 6 slice preparations, p>0.05, paired t-test) (Figs. 6B1-6B2), like we observed after adding SKF-96365 or FFA (Figs. 5B2; 5B2). However, riluzole decreases ∫VRG burst duration (m= 0.48 ± 0.05 and m= 0.41 ± 0.07, in SubP and in SubP + riluzole, n= 6 slice preparations, p<0.05, paired t-test) and frequency (m= 0.44 ± 0.03 and m= 0.40 ± 0.02, in SubP and in SubP + riluzole, n= 6 slice preparations, p<0.01, paired t-test) (Fig. 6B2).

Importantly, in the presence of SubP and riluzole, additionally co-applying SKF-96365 completely eliminates ∫VRG respiratory bursting (Figs. 6C; n= 6 slice preparations; in n=6/6, no rhythmic activity was recorded for >17mins.). The rhythmic ∫VRG bursting during co-application of SubP and riluzole (alone) is more regular (m= 0.27 ± 0.02 and m= 0.16 ± 0.04, before and after perfusion of SubP + riluzole, n= 6 slice preparations, p<0.05, paired t-test) and has a higher frequency (m= 0.23 ± 0.03 and m= 0.40 ± 0.02, before and after perfusion of SubP + riluzole, n= 6 slice preparations, p<0.01, paired t-test) (Figs. 6B1) than control activity (Figs. 6A1) and the bursting area (m= 0.18 ± 0.07 and m= 0.24 ± 0.13, before and after perfusion of SubP + riluzole, n= 6 slice preparations, p>0.05, paired t-test) and duration (m= 0.49 ± 0.03 and m= 0.41 ± 0.07, before and after perfusion of SubP + riluzole, n= 6 slice preparations, p>0.05, paired t-test) are similar to baseline activity (Fig. 6D). Thus, INaP does not appear to be a critical current underlying SubP mediated enhancement of fictive eupnea regularity.

In contrast to INaP-dependent pacemakers, ICAN-dependent pacemaker properties are TRPC channel antagonist sensitive

Our data suggest that SubP enhances ICAN *via* TRPC channels to enhance fictive eupnea. To verify this, we studied the effect of blocking TRPC channels on the SubP-mediated enhancement of synaptically isolated pacemaker bursting activity. As previously shown (Peña and Ramirez, 2004), SubP enhances ICAN-dependent pacemaker burst area and regularity (Figs. 7A1-7A2; and inset ~ red/green overlay). We hypothesized that this enhancement is mediated by TRPC channel activation. Here, we additionally found the ICAN-dependent pacemaker bursting activity is sensitive to TRPC channel antagonists. Indeed, their bursting properties are suppressed within ~5mins after adding SKF-96365 (Fig. 7A3). Longer term (~15min) SKF-96365 application eliminates ICAN-dependent pacemaker bursting properties altogether, such that suprathreshold current injection, initiates action potential spiking, but does not trigger bursting (Fig. 7A4, n=7 neurons). Within 5 minutes of bath application, SKF-96365 inhibits the SubP-mediated increase in bursting irregularity (m= 0.18 ± 0.02 and m= 0.49 ± 0.09, in SubP and in SubP + SKF96365, respectively, n= 7 slice preparations, p<0.05, paired t-test), decreases burst area (m= 1 ± 0.45 and m= 0.24 ± 0.05, in SubP and in SubP + SKF96365, respectively, n= 7 slice preparations, p<0.001, paired t-test) and burst duration (m= 0.74 ± 0.36 and m= 0.41 ± 0.12, in SubP and in SubP + SKF96365, respectively, n= 7 slice preparations, p<0.05, paired t-test) (Fig. 7B; and inset ~ black/ red overlay). The burst frequency is initially elevated after

adding SKF-96365 (m= 0.29 ± 0.07 and m= 0.41 ± 0.07, in SubP and in SubP + SKF96365, respectively, n= 7 slice preparations, p<0.05, paired t-test) (Fig. 7A3), however bursting ceases within ~15mins (n=7 neurons; Figs. 7A1-4; Fig. 7B).

In contrast to ICAN-dependent pacemakers, the bursting of synaptically isolated INaP-dependent pacemakers is not dependent on TRPC channels. Indeed, after INaP-dependent pacemakers are exposed to SubP for 20mins. (Figs. 8A1-8A2; and inset red/green overlay), subsequent SKF-96365 application for 15mins. does not eliminate their bursting properties (Fig. 8A3), as did subsequent application of riluzole (Fig. 8A4; n=3). After pre-exposure to SubP for 20mins. (Figs. 8A1-8A2), additional co-application of SKF-96365 (15mins) to INaP-dependent pacemakers does not alter their bursting irregularity score (m= 0.16 ± 0.03 and m= 0.13 ± 0.02, in SubP and in SubP + SKF96365, respectively, n= 3 slice preparations, p>0.05, paired t-test), their burst area (m= 10 ± 9.61 and m= 7.45 ± 6.64, in SubP and in SubP + SKF96365, respectively, n= 3 slice preparations, p>0.05, paired t-test), their burst duration (m= 0.84 ± 0.16 and m= 1.10 ± 0.31, in SubP and in SubP + SKF96365, respectively, n= 3 slice preparations, p>0.05, paired t-test) and their bursting frequency (m= 0.38 ± 0.06 and m= 0.35 ± 0.05, in SubP and in SubP + SKF96365, respectively, n= 3 slice preparations, p>0.05, paired t-test) (Fig. 8B). In contrast, subsequent application of riluzole eliminates their busting properties (Fig. 8A4), as expected (Peña et al., 2004). Importantly, bath application of SKF-96365 alone (>15mins) does not alter INaP-dependent pacemaker bursting in n=2 additional experiments where SubP was not added (data not shown). These data are consistent with our hypothesis that SubP decreases the irregularity of fictive eupneic network activity and synaptically isolated ICAN-dependent pacemaking via TRPC channel activation.

TRPC channel antagonists block SubP-enhanced inspiratory nonpacemaker bursting during fictive eupnea—We also studied the effect of blocking TRPC channel with SKF-96365 on the SubP-mediated enhancement of nonpacemaker bursting activity during fictive eupnea. During fictive eupnea (Fig. 9A1) we bath-applied 0.1μM SubP for 20mins (Fig. 9A2), then subsequently added SKF-96365 (Fig. 9A3, n= 7 slice preparations). Blocking TRPC channels with SKF-96365 does not eliminate inspiratory non-pacemaker bursting activity (Fig. 9A3, n=7 slice preparations), while subsequent co-application of riluzole stops the network and non-pacemaker bursting activity (Fig. 9A4, n=7 slices preparations; in n=7/7, no rhythmic activity was recorded for >17mins.).

Bath-application of 0.1μM SubP (alone for 20mins) decreases inspiratory non-pacemaker rhythm irregularity (m=0.28 ± 0.03 and m= 0.21 ± 0.02, before and after SubP, respectively, n= 7 slice preparations, p<0.01, paired t-test) and increases burst frequency (m=0.20 ± 0.11 and m= 0.36 ± 0.05, before and after SubP, respectively, n= 7 slice preparations, p<0.01, paired t-test), but does not significantly alter non-pacemaker burst area (m=0.47 ± 0.04 and m= 0.34 ± 0.02, before and after SubP, respectively, n= 7 slice preparations, p>0.05, paired t-test) or burst duration (m=0.39 ± 0.08 and m= 0.29 ± 0.06, before and after SubsP, respectively, n= 7 slice preparations, p>0.05, paired t-test) (Fig. 9B1). After 20mins in SubP, additional co-application of SKF-96265 increases bursting irregularity (m=0.21 ± 0.02 and m= 0.29 ± 0.03, in SubP and in SubP + SKF-96365, respectively, n= 7 slice preparations, p<0.05, paired t-test), decreases burst area underlying action potentials (m=0.34 ± 0.02 and m= 0.41 ± 0.02, in SubP and in SubP + SKF-96365, respectively, n= 7 slice preparations, p<0.01, paired t-test) without altering burst duration (m=0.29 ± 0.06 and m= 0.30 ± 0.08, in SubP and in SubP + SKF-96365, respectively, n= 7 slice preparations, p>0.05, paired t-test) and burst frequency (m=0.36 ± 0.05 and m= 0.25 ± 0.02, in SubP and in SubP + SKF-96365,respectively, n= 7 slice preparations, p>0.05, paired t-test) of inspiratory non-pacemakers (Fig. 9B2). Further, after co-application of SKF-96365, non-pacemaker bursting irregularity (m=0.28 ± 0.03 and m= 0.29 ± 0.03, before and after SubP + SKF-96365,

respectively, *n*= 7 slice preparations, *p*>0.05, paired t-test), burst area (*m*=0.47 ± 0.03 and *m*= 0.41 ± 0.03, before and after SubP + SKF-96365, respectively, *n*= 7 slice preparations, *p*>0.05, paired t-test), burst duration (*m*=0.39 ± 0.08 and *m*= 0.30 ± 0.08, before and after SubP + SKF-96365,respectively, *n*= 7 slice preparations, *p*>0.05, paired t-test) and burst frequency (*m*=0.17 ± 0.03 and *m*= 0.25 ± 0.02, before and after SubP + SKF-96365, *n*= 7 slice preparations, *p*>0.05, paired t-test) are similar to control values measured in ACSF alone (Fig. 9B3, n=7 slice preparations). In contrast to ICAN pacemakers, nonpacemaker bursting activity continues after blocking TRPC channels. These data also suggest that the SubP-mediated enhancement of nonpacemaker activity is reversed by blocking TRPC channels.

Western Blots reveal the expression of TRPC3 and TRPC7 channels in VRG-islands—Our data indicates that SubP-mediated signaling activates a calcium-dependent cation current (ICAN), carried by TRPC channels, to improve the regularity of respiratory activity, *in vitro*. Thus, we made Western Blots to identify which TRPC channels are involved in the SubP-mediated improvement of the respiratory rhythm.

Substance P-mediated signaling positively coupled to Gα/q proteins that will activate phospholipase C (PLC) (Oh et al., 2003). All TRPC channels are activated by PLC pathways, except for TRPC2, which is activated by receptors coupled to Gi/o proteins that inhibit PLC (Clapham, 2007); thus, TRPC2 activity does not underlie the SubP-mediated enhancement of respiratory activity.

Qualitative Western Blots were made to determine the expression of TRPC1, TRPC3, TRPC4, TRPC5, TRPC6 and TRPC7 channels in VRG-islands dissected from 600μm brainslices, after mapping the extent of the pre-BötC/VRG region of rhythmic bursting activity with a population electrode on the surface of the slices from age P8 to P10 mice (Figs. 10A-10B). Our Western Blots also included cortical and cerebellar tissues, isolated from the same mice, as a positive control for the antibodies used. Western-blots revealed the expression of NK1 receptors in VRG-islands (Figs. 10C, n=3 VRG-Islands 1-3). TRPC1 (n=5) channels were detected in the cortex and cerebellum tissue samples, but never in the VRG-islands (Figs. 10D). TRPC3 channels were found in all of the cortical, cerebellar and VRG-island tissues tested (Fig. 10D, n=5). TRPC4 (n=3) channels were detected in the cortex and cerebellum tissue samples, but not in the VRG-islands (Figs. 10D). TRPC5 (n=5) and TRPC6 channels (n=3) were expressed in all of the cortical tissue samples, but was not expressed in the cerebellum or VRG-islands (Fig. 10D). TRPC7 channels are not expressed in the cortex but are expressed in the cerebellum and VRG-islands (Fig.10D, n=5).

Other groups have proposed that ICAN-dependent bursting properties may be mediated by TRPM4 (Crowder et al., 2007; Mironov, 2008). Our data suggests TRPM4 is expressed in the cortex (n=2) and cerebellum (n=2), but TRPM4 is either very weakly expressed or not expressed in VRG-Island preparations (Fig. 10E; n=4). In summary, among TRPC channels, only TRPC3 and TRPC7 were found to be expressed in the VRG-islands where NK1 receptors are also expressed.

Discussion

Substance P is known to improve the regularity of the respiratory rhythm, *in vitro* (Pena and Ramirez, 2004). Here, we demonstrate that SubP signaling leads to activation of TRPC3 and/or TRPC7 (TRPC3/7) channels to improve respiratory rhythm regularity at the network, non-pacemaker and ICAN pacemaker levels. These effects and ICAN pacemaking are blocked by the TRPC3/7 channel antagonists, either SKF-96365 or FFA (Figs. 3; 4).

Our data show that SubP, *via* NK1 receptors, selectively increases ICAN-dependent intrinsic bursting mechanisms to enhance fictive eupneic regularity (Fig. 7). Indeed, blocking ICAN with FFA, reverses or prevents SubP-mediated enhancement of fictive eupneic regularity (Figs. 4 and 5). In contrast, blocking INaP with riluzole, did not reverse SubP-mediated enhancement of fictive eupnea regularity (Fig. 6).

Combined bath-application of FFA and riluzole eliminates respiratory rhythm bursting mechanisms (Peña et al., 2004). Here, we show that SKF-96365 also blocks ICAN-dependent intrinsic bursting and sensitizes the ventral respiratory group (VRG) population rhythm to riluzole. In contrast, SKF-96365 does not block INaP-dependent intrinsic bursting properties nor does SKF-96365 reverse the SubP-mediated enhancement of INaP-dependent pacemaker bursting (Fig. 9) (Peña and Ramirez, 2004).

SubP is known to activate TRPC3 channels (Oh et al., 2003). Here, we demonstrate that in VRG-islands, TRPC3 and TRPC7 channels are expressed (Fig. 10). Thus, we propose that ICAN-dependent endogenous bursting is mediated *via* TRPC3/7 channels, as we reverse the effects of SubP modulation of ICAN-dependent bursting properties with TRPC3/7 channel antagonists. Currently, there are no commercially available selective TRPC3 or TRPC7 channel antagonists to precisely distinguish between the contribution of these channels to the respiratory rhythm regularity.

Rhythmic activity in the VRG has been previously hypothesized to depend in part on TRPM4/5 (Crowder et al., 2007; Mironov, 2008). To our knowledge, SubP is not known to activate TRPM channels and we were unable to detect TRPM4 protein expression in Western blots made from VRG-island preparations. Thus, either TRPM4 proteins are: 1) not expressed in the VRG-Is in CD-1 mice (age P8); 2) or TRPM4 expression is very low in the VRG; as we did not detect TRPM4 at 10μg/mL or 50μg/mL total protein; 3) or the TRPM4 antibodies we used were non-competent. As the antibody we used appears to recognize TRPM4 expression in the cortex and cerebellum, but not the VRG-island (at 10μg/mL total protein), the third possibility is unlikely.

It was proposed that SubP modulates a TTX-R background sodium current to enhance respiratory pacemaker bursting properties (Peña and Ramirez, 2004). We also previously found that a reduction in background sodium currents results in irregular inspiratory network and pacemaker bursting (Tryba and Ramirez, 2004b; Chevalier et al., 2008). Indeed, SubP signaling activates TRPC3 channels, that largely carry a TTX-R sodium current (Zhou et al., 2008) and here our data suggest that SubP modulation of TRPC3/7 channel currents enhances respiratory network and pacemaker bursting regularity. Canonical transient receptor proteins, such as TRPC channels, depend on a rise in intracellular calcium for full activation, that would typically be augmented during an ongoing burst of action potentials (Oh et al. 2003; Clapham, 2007). It should be noted that TRPC channels are additionally associated with intracellular calcium oscillations (Rey et al., 2006) and our study suggests TRPC3/7 channels are well suited to underlie and/or amplify intrinsic bursting properties to alter the regularity of breathing activity.

A dysregulation of TRPC3 channels has been implicated in Rett Syndrome (Deguchi et al., 2000), in which an irregular breathing rhythmogenesis is typical (Viemari et al., 2005a). Our data suggest that a dysfunction in TRPC3/7 channel activation may result in irregular breathing activity. In our study, we demonstrated the activation of TRPC3/7 by synaptically released SubP-signaling improves the respiratory rhythm regularity. These data do not exclude the possible contribution of other neuromodulators that can activate TRPC channels, such as BDNF (Bouvier et al., 2008). Dysregulation of BDNF signaling has been

hypothesized to underlie the functional and structural consequences of MeCP2 mutations in Rett Syndrome (Amaral et al., 2007).

Acknowledgments

Authors thank Sandra Chuppa and Christine Puza for technical support and Drs. Bert Forster and Catherine Kaczorowski for editing the manuscript prior to submission. Supported by NIH R01HL079294 and R01HL079294-04S1 (to AKT) from the National Heart, Lung, And Blood Institute.

Abbreviations

pre-BötC	pre-Bötzinger Complex
VRG	Ventral Respiratory Group
SIDS	Sudden Infant Death Syndrome
TRPC3	Transient receptor protein canonical 3
TRPC7	Transient receptor protein canonical 7

Literature Cited

Amaral MD, Pozzo-Miller L. BDNF Induces Calcium Elevations Associated With IBDNF, a Nonselective Cationic Current Mediated by TRPC Channels. J Neurophysiol 2007;98:2476–2482. [PubMed: 17699689]

Amaral MD, Chapleau CA, Pozzo-Miller L. Transient receptor potential channels as novel effectors of brain-derived neurotrophic factor signaling: Potential implications for Rett syndrome. Pharmacology & Therapeutics 2007;113:394–409. [PubMed: 17118456]

Barthe JY, Clarac F. Modulation of the spinal network for locomotion by substance P in the neonatal rat. Experimental Brain Research 1997;115:485–492.

Boesmans W, Gomes P, Janssens J, Tack J, Berghe PV. Brain-derived neurotrophic factor amplifies neurotransmitter responses and promotes synaptic communication in the enteric nervous system. Gut 2008;57:314–322. [PubMed: 17965066]

Bouvier J, Autran S, Dehorter N, Katz DM, Champagnat J, Fortin G, Thoby-Brisson M. Brain-derived neurotrophic factor enhances fetal respiratory rhythm frequency in the mouse preBötzinger complex *in vitro*. European Journal of Neuroscience 2008;28:510–520. [PubMed: 18702723]

Chevalier M, Ben-Mabrouk F, Tryba AK. Background sodium current underlying respiratory rhythm regularity. European Journal of Neuroscience 2008;28:2423–2433. [PubMed: 19032590]

Clapham DE. TRP channels as cellular sensors. Nature 2003;426:517–524. [PubMed: 14654832]

Clapham DE. SnapShot: mammalian TRP channels. Cell 2007;129:220. [PubMed: 17418797]

Crowder EA, Saha MS, Pace RW, Zhang H, Prestwich GD, Del Negro CA. Phosphatidylinositol 4,5-bisphosphate regulates inspiratory burst activity in the neonatal mouse preBotzinger complex. J Physiol 2007;582:1047–1058. [PubMed: 17599963]

Deguchi K, Antalffy BA, Twohill LJ, Chakraborty S, Glaze DG, Armstrong DD. Substance P immunoreactivity in Rett syndrome. Pediatr Neurology 2000;22:259–266.

Feldman MJ, Morris GP, Paterson WG. Role of Substance P and Calcitonin Gene-Related Peptide in Acid-Induced Augmentation of Opossum Esophageal Blood Flow. Digestive Diseases and Sciences 2001;46:1194–1199. [PubMed: 11414293]

Gray PA, Rekling JC, Bocchiaro CM, Feldman JL. Modulation of Respiratory Frequency by Peptidergic Input to Rhythmogenic Neurons in the PreBotzinger Complex. Science 1999;286:1566–1568. [PubMed: 10567264]

Grillner S. Biological Pattern Generation: The Cellular and Computational Logic of Networks in Motion. Neuron 2006;52:751–766. [PubMed: 17145498]

Johnson SM, Koshiya N, Smith JC. Isolation of the Kernel for Respiratory Rhythm Generation in a Novel Preparation: The Pre-Botzinger Complex “Island”. J Neurophysiol 2001;85:1772–1776. [PubMed: 11287498]

Jun JY, Choi S, Yeum CH, Chang IY, You HJ, C.K. P, Kim MY, Kong ID, Kim MJ, Lee KP, So I, Kim KW. Substance P induces inward current and regulates pacemaker currents through tachykinin NK1 receptor in cultured interstitial cells of Cajal of murine small intestine. Eur J Pharmacol 2004;495:35–42. [PubMed: 15219818]

Kozlov A, Kotaleski JH, Aurell E, Grillner S, Lansner A. Modeling of Substance P and 5-HT Induced Synaptic Plasticity in the Lamprey Spinal CPG: Consequences for Network Pattern Generation. Journal of Computational Neuroscience 2001;11:183–200. [PubMed: 11717534]

Lekman A, Witt-Engerström I, Gottfries J, Hagberg BA, Percy AK, Svennerholm L. Rett syndrome: biogenic amines and metabolites in postmortem brain. Pediatr Neurology 1989;5:357–362.

Lieske SP, Thoby-Brisson M, Telgkamp P, Ramirez JM. Reconfiguration of the neural network controlling multiple breathing patterns: eupnea, sighs and gasps. Nat Neurosci 2000;3:600–607. [PubMed: 10816317]

Matsuishi T, Nagamitsu S, Yamashita Y, Murakami Y, Kimura A, Sakai T, Shoji H, Kato H, Percy AK. Decreased cerebrospinal fluid levels of substance P in patients with Rett syndrome. Ann Neurol 1997;42:978–981. [PubMed: 9403492]

Mironov SL. Metabotropic glutamate receptors activate dendritic calcium waves and TRPM channels which drive rhythmic respiratory patterns in mice. J Physiol 2008;586:2277–2291. [PubMed: 18308826]

Oh EJ, Gover TD, Cordoba-Rodriguez R, Weinreich D. Substance P Evokes Cation Currents Through TRP Channels in HEK293 Cells. J Neurophysiol 2003;90:2069–2073. [PubMed: 12966182]

Pearlstein E, Mabrouk F Ben, Pflieger J, Vinay L. Serotonin refines the locomotor-related alternations in the in vitro neonatal rat spinal cord. European Journal of Neuroscience 2005;21:1338–1346. [PubMed: 15813943]

Pena F, Ramirez J-M. Substance P-Mediated Modulation of Pacemaker Properties in the Mammalian Respiratory Network. J Neurosci 2004;24:7549–7556. [PubMed: 15329402]

Peña F, Ramirez J-M. Substance P-Mediated Modulation of Pacemaker Properties in the Mammalian Respiratory Network. J Neurosci 2004;24:7549–7556. [PubMed: 15329402]

Peña F, Parkis MA, Tryba AK, Ramirez J-M. Differential Contribution of Pacemaker Properties to the Generation of Respiratory Rhythms during Normoxia and Hypoxia. Neuron 2004;43:105–117. [PubMed: 15233921]

Rey O, Young SH, Papazyan R, Shapiro MS, Rozengurt E. Requirement of the TRPC1 Cation Channel in the Generation of Transient Ca2+ Oscillations by the Calcium-sensing Receptor. J Biol Chem 2006;281:38730–38737. [PubMed: 17046820]

Ruangkittisakul A, Schwarzacher SW, Secchia L, Ma Y, Bobocea N, Poon BY, Funk GD, Ballanyi K. Generation of Eupnea and Sighs by a Spatiochemically Organized Inspiratory Network. J Neurosci 2008;28:2447–2458. [PubMed: 18322090]

Saideman SR, Blitz DM, Nusbaum MP. Convergent Motor Patterns from Divergent Circuits. J Neurosci 2007;27:6664–6674. [PubMed: 17581953]

Segawa M. Pathophysiology of Rett syndrome from the standpoint of early catecholamine disturbance. Eur Child Adolesc Psychiatry 1997;6:56–60. [PubMed: 9452921]

Shvarev Y, Lagercrantz H, Yamamoto Y. Biphasic effects of substance P on respiratory activity and respiration-related neurones in ventrolateral medulla in the neonatal rat brainstem in vitro. Acta Physiologica Scandinavica 2002;174:67–84. [PubMed: 11851598]

Smith J, Ellenberger H, Ballanyi K, Richter DW, Feldman JL. Pre-Bötzinger complex: a brainstem region that may generate respiratory rhythm in mammals. Science Nov 1;1991a 254:726–729. [PubMed: 1683005]

Smith JC, Ellenberger HH, Ballanyi K, Richter DW, Feldman JL. Pre-Botzinger Complex: a brainstem region that may generate respiratory rhythm in mammals. Science 1991b;254:726. [PubMed: 1683005]

St.-John WM, Rudkin AH, Harris MR, Leiter JC, Paton JFR. Maintenance of eupnea and gasping following alterations in potassium ion concentration of perfusates of in situ rat preparation. Journal of Neuroscience Methods 2005;142:125–129. [PubMed: 15652625]

Telgkamp P, Cao YQ, Basbaum AI, Ramirez J-M. Long-Term Deprivation of Substance P in PPT-A Mutant Mice Alters the Anoxic Response of the Isolated Respiratory Network. J Neurophysiol 2002;88:206–213. [PubMed: 12091546]

Thoby-Brisson M, Simmers J. Neuromodulatory Inputs Maintain Expression of a Lobster Motor Pattern-Generating Network in a Modulation-Dependent State: Evidence from Long-Term Decentralization In Vitro. J Neurosci 1998;18:2212–2225. [PubMed: 9482805]

Thoby-Brisson M, Ramirez J-M. Identification of Two Types of Inspiratory Pacemaker Neurons in the Isolated Respiratory Neural Network of Mice. J Neurophysiol 2001;86:104–112. [PubMed: 11431492]

Tryba AK, Ramirez J-M. Hyperthermia Modulates Respiratory Pacemaker Bursting Properties. J Neurophysiol 2004a;92:2844–2852. [PubMed: 15190095]

Tryba AK, Ramirez JM. Background sodium current stabilizes bursting in respiratory pacemaker neurons. Journal of Neurobiology 2004b;60:481–489. [PubMed: 15307152]

Tryba AK, Pena F, Ramirez J-M. Stabilization of Bursting in Respiratory Pacemaker Neurons. J Neurosci 2003;23:3538–3546. [PubMed: 12716963]

Tryba AK, Pena F, Ramirez J-M. Gasping Activity In Vitro: A Rhythm Dependent on 5-HT2A Receptors. J Neurosci 2006;26:2623–2634. [PubMed: 16525041]

Tryba AK, Pena F, Lieske SP, Viemari J-C, Thoby-Brisson M, Ramirez J-M. Differential Modulation of Neural Network and Pacemaker Activity Underlying Eupnea and Sigh-Breathing Activities. J Neurophysiol 2008;99:2114–2125. [PubMed: 18287547]

Viemari J-C, Roux J-C, Tryba AK, Saywell V, Burnet H, Pena F, Zanella S, Bevengut M, Barthelemy-Requin M, Herzing LBK, Moncla A, Mancini J, Ramirez J-M, Villard L, Hilaire G. Mecp2 Deficiency Disrupts Norepinephrine and Respiratory Systems in Mice. J Neurosci 2005a; 25:11521–11530. [PubMed: 16354910]

Viemari JC, Roux JC, Tryba AK, Saywell V, Burnet H, Pena F, Zanella S, Bevengut M, Barthelemy-Requin M, Herzing LB, Moncla A, Mancini J, Ramirez JM, Villard L, Hilaire G. Mecp2 deficiency disrupts norepinephrine and respiratory systems in mice. J Neurosci 2005b;25:11521–11530. [PubMed: 16354910]

Zhou F-W, Matta SG, Zhou F-M. Constitutively Active TRPC3 Channels Regulate Basal Ganglia Output Neurons. J Neurosci 2008;28:473–482. [PubMed: 18184790]

Zoghbi HY, Milstien S, Butler IJ, Smith EO, Kaufman S, Glaze DG, Percy AK. Cerebrospinal fluid biogenic amines and biopterin in Rett syndrome. Ann Neurol 1989;25:56–60. [PubMed: 2913929]

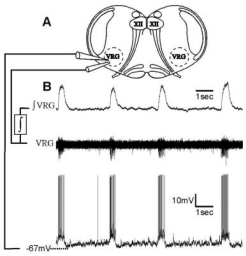

Figure 1. Mouse medullary slice preparation containing the neural network for respiratory activity generation

A) Extracellular electrodes were placed on the surface of the VRG to record population activity. Intracellular electrodes were placed close to the extracellular electrodes to simultaneously record inspiratory neuron activity. **B)** Raw VRG population activity was integrated (∫); the integrated VRG activity is dominated by inspiratory neurons, giving rise to fictive inspiratory bursts in the integrated traces (∫VRG). Lower trace is a simultaneous intracellular recording of inspiratory neuron bursting in phase with the population.

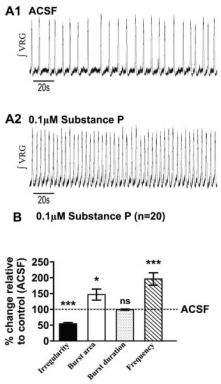

Figure 2. Substance P enhances the fictive eupneic rhythm generated by the ventral respiratory group (∫VRG)

A1) Fictive eupnea (∫VRG) recorded in control condition (ACSF) and after **A2)** bath application of 0.1 μM SubP. **B)** SubP decreases the fictive eupneic, ∫VRG burst irregularity while it enhances the burst area and increases the burst frequency (*, $p<0.05$ and *** $p<0.001$, paired t-test), without altering burst duration (statistical tests were made on raw data).

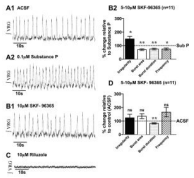

Figure 3. Substance P enhances respiratory rhythm *via* canonical transient receptor protein (TRPC) channels

A1) Fictive eupneic activity (∫VRG) recorded in control condition (ACSF) and after **A2**) bath application of 0.1 μM SubP. **B1**) In the presence of SubP, subsequent bath application of 5-10μM SKF-96365, suppresses the SubP enhancement of VRG rhythm by SubP within ~10-15mins). **B2**) In the presence of SubP, subsequent bath application of SKF-96365 increases the burst irregularity and decreases the burst area, the burst duration and the rhythm frequency (*, $p<0.05$; **, $p<0.01$, paired t-test). **C)** In the presence of SubP and SKF-96365, additionally blocking the persistent sodium current (INaP) with 10μM of riluzole abolished the VRG respiratory rhythm. **D**) Following 20mins of SubP bath-application, subsequent co-application of SKF-96365 increased ∫VRG bursting irregularity, while burst area and frequency were similar to control values (ACSF), burst duration was reduced (**, $p<0.01$, paired t-test) (statistical tests were made on raw data).

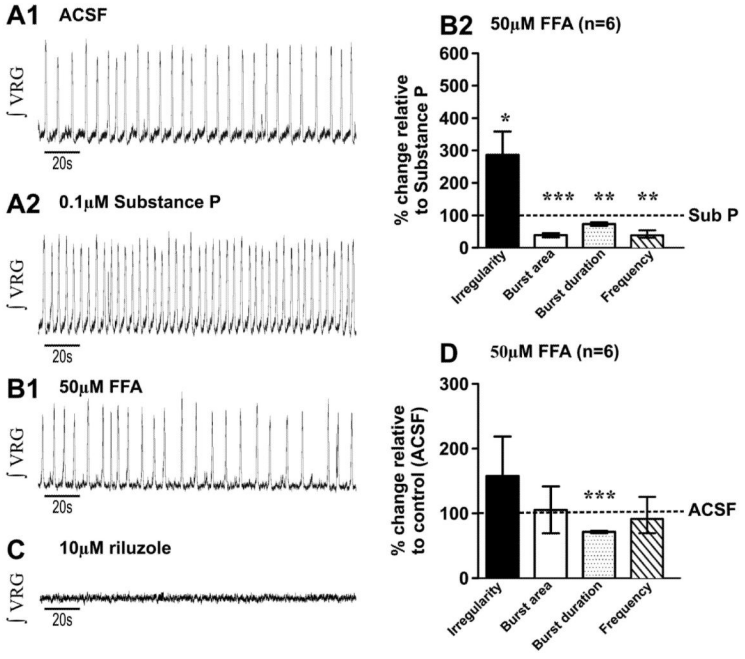

Figure 4. Flufenamic acid reverses the improvement of the respiratory rhythm by the Substance P

A1) Fictive eupneic activity (∫VRG) recorded in control (ACSF); and **A2)** following bath application of 0.1 μM SP for 20mins. **B1)** In the presence of SubP, subsequent bath application of 50μM of flufenamic acid (FFA) **B2)** reverses the SubP respiratory rhythm enhancement by increasing the rhythm irregularity and decreasing the burst area, the burst duration and the rhythm frequency (*, $p<0.05$; **, $p<0.01$; ***, $p<0.001$ paired t-test). **C)** In the presence of SubP and SKF-96365, subsequent additional application of 10μM riluzole completely abolished the ∫VRG rhythm. **D)** Following SubP bath- application for 20 mins., co-application of FFA, the ∫VRG bursting irregularity, burst area and frequency were similar to control values (ACSF only), while burst duration was reduced (***, $p<0.001$ paired t-test) (statistical tests were made on raw data).

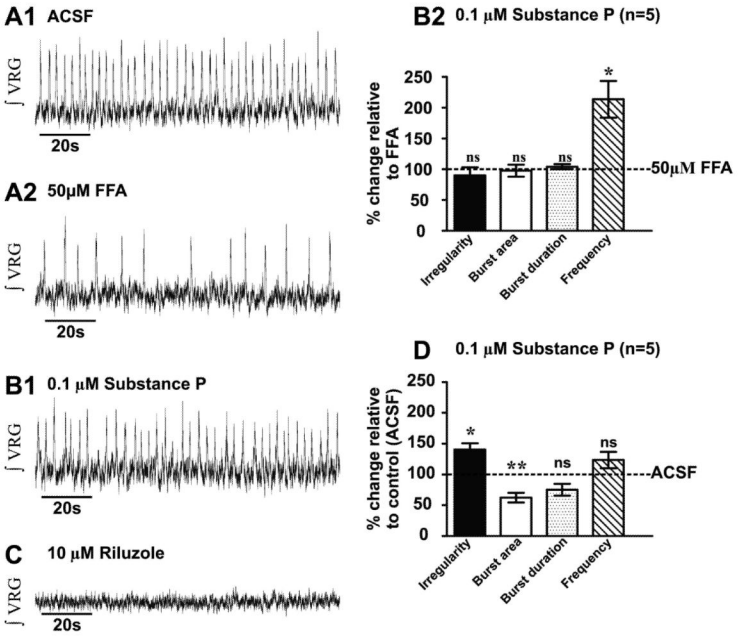

Figure 5. Flufenamic acid prevents modulation of fictive eupnea (∫VRG) via Substance P

A1) Fictive eupneic activity (∫VRG) recorded in control condition (ACSF) and after **A2**) bath-application of FFA (50μM for 30 mins). **B1)** Pretreatment with FFA prevented the SubP enhancement of the fictive eupnea. **B2)** In the presence of FFA, subsequent bath co-application of SubP fails in improve the regularity, enhance the burst area and prolong the burst duration. However, an increase of the frequency (*, $p<0.05$; paired t-test) is observed. **C)** During FFA and SubP co-application, additional application of 10μM riluzole completely abolished the ∫VRG rhythm. **D)** After FFA-preincubation, rather than enhancing respiratory activity, subsequent SubP application resulted in ∫VRG rhythmic activity being more irregular, with a reduced burst area, while burst duration and frequency were similar, relative to control values (ACSF only) (*, $p<0.05$; **, $p<0.01$, paired t-test) (statistical tests were made on raw data).

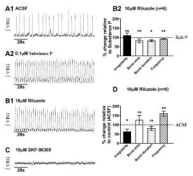

Figure 6. The enhancement of respiratory rhythm regularity by Substance P does not involve the persistent sodium current (INaP)

A1) Fictive eupneic activity (∫VRG) recorded in control conditions (ACSF) and after **A2)** bath-application of SubP (20 mins). **B1)** In the presence of SubP, subsequent bath application of 10μM of riluzole for 10mins. **B2)** does not affect the SubP-mediated decrease in fictive eupnea irregularity and enhanced burst area (see also Fig. 3). Only the burst duration and the frequency are decreased (*, $p<0.05$; **, $p<0.01$, paired t-test). **C)** In the presence of SubP and riluzole, subsequently adding 10μM of SKF96365 disrupts, then abolishes, the rhythm. **D)** In the presence of SubP and riluzole (Fig. 7B1), ∫VRG rhythmic activity is less irregular and has a higher frequency, while burst area and burst duration were similar to control values (ACSF only, Fig. 7A1, *, $p<0.05$; **, $p<0.01$, paired t-test) (statistical tests were made on raw data).

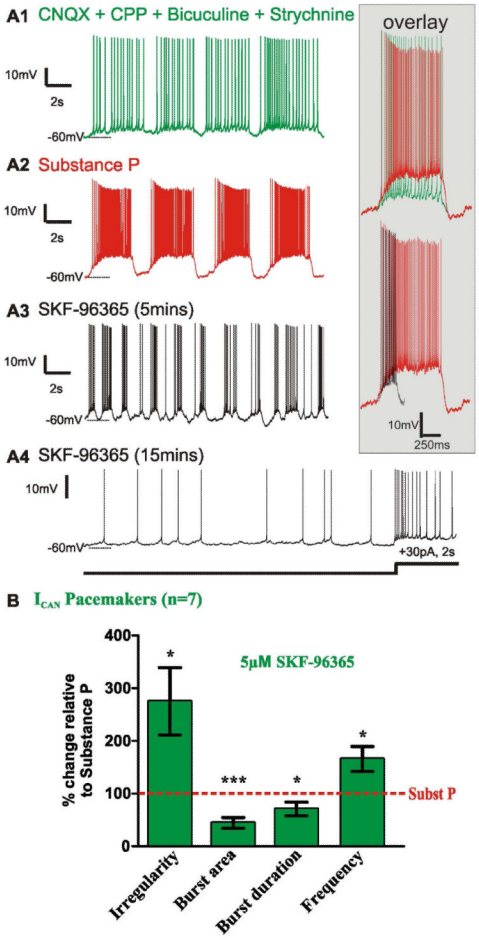

Figure 7. Calcium-dependant cation current (ICAN) is carried by TRPC3/7 channels

A1) ICAN pacemaker neuron activity recorded while bath-applying a mixture of synaptic antagonists, CNQX, CPP, bicuculine, strychnine. **A2**) SubP (0.1µM) enhances ICAN pacemaker bursting properties (green/red overlay) (Pena and Ramirez 2002). **A3**) Following 20mins. bath application of SubP, subsequent co-application of SKF96365 (5µM), an antagonist of canonical transient receptor protein (TRPC) channels, reverses the SubP-enhanced bursting properties, within 5 mins. (red/black overlay). **A4)**, A longer term (~15min) perfusion SKF-96365 abolishes ICAN pacemaker bursting properties. After SKF-96365 application, depolarizing current injection did not trigger bursting activity (30pA steps, 2sec duration). **B**) After 20mins in SubP, subsequent co-application of SKF-96365, for 5mins. initially leads to an increase in the burst irregularity, decrease in the burst area, while the burst duration is initially the same as in SubP, while burst frequency is increased prior to reducing then eliminating bursting (*, $p<0.05$; ***, $p<0.001$, paired t-test) (statistical tests were made on raw data).

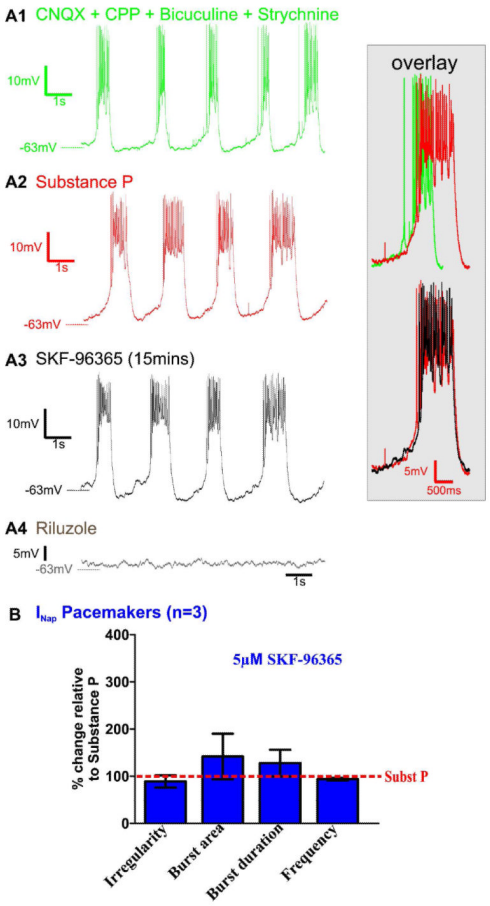

Figure 8. Persistent sodium current (INaP) pacemaking is not TRPC channel dependent

A1) INaP-dependent pacemaker neuron activity recorded while bath-applying a mixture of CNQX, CPP, bicuculine, strychnine. **A2)** Bath application of SubP (0.1µM, 20mins.) enhances INaP)-dependent pacemaker activity bursting properties (green/red overlay). **A3)** In the presence of SubP, subsequent bath application of SKF-96365 (5µM) 15mins),, does not block SubP-enhanced rhythmic bursting of INaP-dependent pacemakers (red/black overlay). **A4)** As expected, INaP-dependent pacemaker bursting properties are abolished within 10mins. following additionally applying riluzole 10µM. **B)** In the presence of SubP, the burst irregularity, the burst area, the burst duration or the frequency were not affected by subsequently adding SKF-96365 (statistical tests were made on raw data).

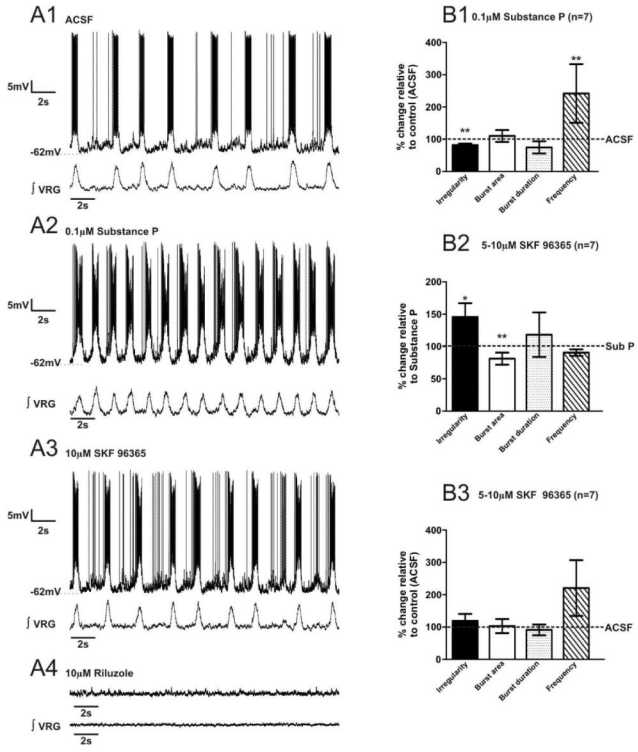

Figure 9. SubP-enhancement of inspiratory non-pacemaker activity is reversed by SKF-96365

A1) Fictive eupneic activity (∫VRG) and inspiratory non-pacemaker neuron recorded in control conditions (ACSF) and after **A2)** bath-application of SubP (20 mins). **A3)** In the presence of SubP. subsequent bath co-application of SKF-96365 does not eliminate ∫VRG and inspiratory non-pacemaker bursting properties, while **A4)** subsequent additional co-application of riluzole eliminates inspiratory non-pacemaker rhythmic bursting. **B1)** SubP application decreases inspiratory non-pacemaker rhythm irregularity and increases burst frequency but did not significantly alter burst area or burst duration (*, $p<0.05$, paired t-test). **B2)** After 20mins. in SubP, subsequent co-application of SKF-96365 increased bursting irregularity, decreased burst area underlying action potentials and decreased burst frequency, without altering burst duration of inspiratory non-pacemakers (*, $p<0.05$, paired t-test). **B3)** Following 20mins of SubP bath-application, subsequent co-application of SKF-96365, non-pacemaker bursting irregularity, burst area, burst duration and burst frequency were similar to control values measured in ACSF alone (statistical tests were made on raw data).

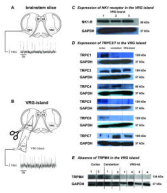

Figure 10. Qualitative Western blots reveal the expression of canonical transient receptor proteins 3 and 7 (TRPC3 and TRPC7) in the VRG

A) ∫VRG activity recorded from the whole medullary slice, in control conditions (ACSF). **B)** ∫VRG activity recorded from the VRG-island after its isolation from the rest of the medullary slice, in control conditions (ACSF). **C)** NK1 receptors (10μg total protein/ lanes 1-3); and, **D)** TRPC1 channels are expressed in the cortex, but not in the cerebellum or VRG-island preparations, 15μg total protein/ lanes). TRPC3 channels are expressed in all the VRG-islands tested (15μg total protein/ lanes 1-3). TRPC4 channels are expressed in the cortex and cerebellum but not the VRG-islands, (15μg total protein/ lanes), whereas TRPC5 channels (15μg total protein/ lanes) and TRPC6 channels preparations, 15μg total protein/ lanes) are expressed in the cortex and, but not in the cerebellum or VRG-islands. TRPC7 channels are expressed in the cerebellum and VRG-islands (15μg total protein/ lanes). **E**) TRPM4 channels were detected in the cortex (10μg total protein/ lanes 1 and 2) and cerebellum (10μg total protein/ lanes 1 and 2) but does not appear to be expressed in the VRG-Island (VRG-Island preparations; 10μg total protein/ lanes 1 and 3; 50μg total protein/ lanes 2 and 4).